Atomic Interferometry with the Micromaser

G. Raithel, O. Benson, and H. Walther
Sektion Physik der Universität München and Max-Planck-Institut für Quantenoptik, 85748 Garching, Federal Republic of Germany
(Received 3 August 1995)

Atomic interferences are observed in the micromaser when the inversion of the atoms leaving the cavity is measured while the cavity frequency is scanned across the atomic resonance. The interferences are due to the nonadiabatic mixing of dressed states at the entrance and exit holes of the maser cavity. The interference structures are triangular shaped and approximately equidistant. They are associated with the dynamics of the atom-field interaction, show quantum jumps, and demonstrate bistability of the micromaser field.

PACS numbers: 42.52.+x, 32.80.–t, 42.50.Lc

The one-atom maser or micromaser allows one to study the resonant interaction of a single atom with a single mode of a superconducting niobium cavity [1–4]. In previous experiments values of the quality factor as high as 3×10^{10} have been achieved for the resonant mode, corresponding to an average lifetime of a photon in the cavity of 0.2 s. The photon lifetime is thus much longer than the interaction time of an atom with the maser field. The atoms used in the experiments are rubidium Rydberg atoms pumped by laser excitation into the upper level of the maser transition, which is usually induced between neighboring Rydberg states. In the experiments, the atom-field interaction is probed by observing the population in the upper and lower maser levels after the atoms have left the cavity. The field in the cavity consists only of single or a few photons. Nevertheless, it is possible to study the interaction in considerable detail. Thus, the dynamics of the atom-field interaction treated with the Jaynes-Cummings model was investigated by selecting and varying the velocity of the pump atoms [2]. The counting statistics of the pump atoms emerging from the cavity allowed one to measure the nonclassical character of the cavity field [3,4], and recently it was observed that under suitable experimental conditions the maser field exhibits bistability and hysteresis [5].

In this paper we report on the observation of the maser resonance under conditions where atomic interference phenomena in the cavity become observable. Since a nonclassical field is generated in the maser cavity, we are able to investigate for the first time atomic interference phenomena under the influence of nonclassical radiation; owing to the bistable behavior of the maser field the interferences display quantum jumps, thus the quantum nature of the field becomes directly visible in the interference fringes. Interferences occur since a coherent superposition of the combined atom-field states (dressed states) is produced by mixing the states at the entrance and exit holes of the cavity. This leads to interferences that are similar to those observed in a separated two-field interaction known as Ramsey interferences [6].

The setup used in the experiment is identical to the one described previously [5]. However, the flux of atoms through the cavity is a factor of 5–10 higher than in the previous experiments, where we also used the $63P_{3/2}$-$61D_{5/2}$ transition. The atoms are excited into the upper maser level, $63P_{3/2}$, shortly before they enter the cylindrical cavity. The velocity of the atoms can be selected by exciting a velocity subgroup. Behind the cavity the atoms are detected in separate detectors for upper and lower maser levels. The Q- value of the cavity, cooled to 0.1 K, was 6×10^9 corresponding to a photon decay time of 42 ms.

Figure 1 shows the standard maser resonance in the uppermost plot that is obtained when the resonator frequency is tuned. At large values of N_{ex} ($N_{ex} > 89$) sharp,

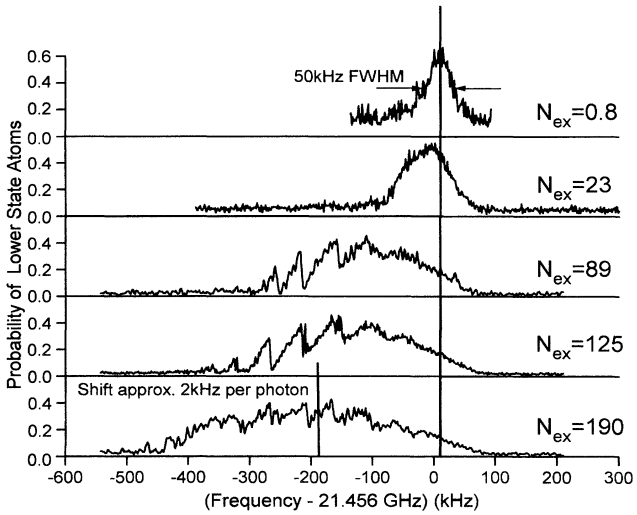

FIG. 1. Shift of the maser resonance $63P_{3/2}$-$61D_{5/2}$ for fast atoms ($t_{int} = 35\ \mu s$). The upper plot shows the maser line for low pump rate ($N_{ex} < 1$). The FWHM linewidth (50 kHz) sets an upper limit of $\approx$5 mV/cm to residual stray electric fields in the center of the cavity. The lower resonance lines are taken for the indicated large values of N_{ex}. The plots show that the center of the maser line shifts by about 2 kHz per photon. In addition, there is considerable field-induced line broadening which is approximately proportional to $\sqrt{N_{ex}}$. For $N_{ex} \geq 89$ the lines display periodic structures, which are discussed in the text.

 0031-9007/95/75(19)/3446(4)$06.00

periodic structures appear. These typically consist of a smooth wing on the low-frequency side, and a vertical step on the high-frequency side. The visibility of the pattern rapidly decreases when N_{ex} increases to 190 or beyond. We will see later that these structures have to be interpreted as interferences. It can be seen that the atom-field resonance frequency is redshifted with increasing N_{ex}, the shift reaching 200 kHz for $N_{ex} = 190$. Under these conditions there are roughly 100 photons, on the average, in the cavity. The large redshift cannot be explained by the ac Stark effect, which for 100 photons would amount to about 1 kHz for the transition used. Therefore it is obvious that other reasons must be responsible for the observed shift.

It is known from previous maser experiments (e.g., [5]) that there are small static electric fields in the entrance and exit holes of the cavity. It is supposed that this field is generated by patch effects at the surface of the niobium metal caused by rubidium deposits caused by the atomic beam or by microcrystallites formed when the cavities are tempered after machining. The influence of those stray fields is only observable in the cavity holes; in the center of the cavity they are negligible owing to the large atom-wall distances.

Figure 2 shows the variation of the structure when the interaction time t_{int} between the atoms and the cavity field is changed. The substructure disappears for $t_{int} > 47\ \mu s$. In the second plot from the top a substructure is still present on the left side, but it is less pronounced than in the uppermost one. Furthermore, an increasing shift of the whole structure to low frequencies is observed when t_{int} is increased.

In order to understand the observed phenomena, we first have to analyze the atom-field interaction. The basis is the Jaynes-Cummings operator, which describes the interaction of a single mode of a quantized field with a single atom, leading to the dressed states as eigenstates [7]. Through the interaction the coupled atom-field states split depending on the vacuum Rabi-flopping frequency Ω, the photon number n, and the atom-field detuning δ. We face a special situation at the entrance and exit holes of the cavity. There we have a position-dependent variation of the cavity field, as a consequence of which Ω is position dependent. An additional variation results from the stray electric fields in the entrance and exit holes. Owing to the Stark effect, which differently affects the upper and lower maser states, these fields lead to a position-dependent atomic transition frequency.

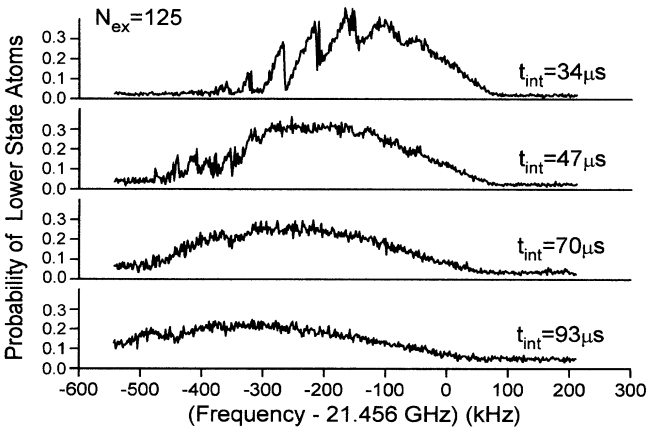

FIG. 2. Maser resonance lines for large N_{ex} and the indicated values of t_{int}. The period and clarity of the additional structures reduce when t_{int} is increased. Furthermore, the center of the resonance shifts to lower frequency with increasing t_{int}.

The interaction only couples pairs of dressed states. Therefore, it is sufficient to consider the dynamics within such a pair. In our case, prior to the atom-field interaction the system is in one of the two dressed states. For experimental parameters where the periodic substructures in Figs. 1 and 2 are observed the dressed states are mixed only at the beginning of the atom-field interaction and at the end. The mixing is due to a crossing of the dressed states energy levels at a location where the position-dependent atomic transition frequency equals the cavity resonance frequency. At this location the repulsion of the dressed states, which is proportional to the maser field strength, determines whether this crossing is passed more or less adiabatically, i.e., whether a transition from one dressed state to the other one is impossible or possible. The crossing at the beginning creates a coherent superposition of the dressed states. Afterwards the system develops adiabatically, whereby the two dressed states accumulate a differential dynamic phase Φ, which strongly depends on the cavity frequency.

The mixing of the dressed states at the entrance and exit holes of the cavity, in combination with the intermediate adiabatic evolution, generates a situation similar to a Ramsey two-field interaction [6]. In a Ramsey two-field interaction a coherent superposition of two atomic levels is generated in two spatially separated interaction zones. Interferences occur due to the two possible "paths": transition in the first or second zone.

In order to explain the observed periodic substructures a quantitative calculation on the basis of the micromaser theory [8,9] can be performed in the following way. First, the variation of the static electric field in the cavity has to be estimated. This is done by numerically solving the Laplace equation with the boundaries of the cavity and assuming a particular field strength in the cavity holes. Then for different interaction times, photon numbers, and cavity frequencies the dynamics of the atom-field wave function is calculated by numerical integration based on the Jaynes-Cummings model. This integration has to include the local variation of Ω inside the cavity owing to the mode structure of the microwave field (in our case the TE_{121} mode). Furthermore, the variation of the detuning δ resulting from the static electric fields in the cavity holes has to be considered. In order to use the micromaser model, we extract the values β_n, which

denote the probabilities of an atom emitting a photon in a field of $n - 1$ photons prior to the interaction.

In the second step of the calculation, with the values of β_n the photon number distribution $P(n)$ of the cavity field under steady-state conditions is obtained from the recursion formula

$$P(n) = \frac{n_b}{n_b + 1}\left(1 + \frac{N_{\mathrm{ex}}\langle\beta_n\rangle}{nn_b}\right)P(n-1).$$

Here n_b stands for the number of thermal photons. The $\langle\,\rangle$ indicate that the β_n have to be averaged over all statistical fluctuations such as the spread of t_{int} caused by the velocity distribution. The fact that the atoms pass in slightly different directions through the cavity holes and thus experience slightly different stray fields is also included in the averaging. The latter phenomenon may lead to a disappearance of the interferences for long t_{int} and large N_{ex}. With $P(n)$ the normalized average photon number $\langle n\rangle/N_{\mathrm{ex}}$ is calculated. This quantity corresponds to the probability of finding an atom in the lower state, as do the experimental results displayed in Figs. 1 and 2.

A theoretial result of $\langle n\rangle/N_{\mathrm{ex}}$ obtained in this way is shown in Fig. 3. The uppermost plot shows the maser resonance line expected without any static electric field. With increasing dc field strength in the cavity holes the structure changes, the curve for 309 mV/cm coming very close to those displayed in Fig. 1 for $N_{\mathrm{ex}} = 89$ and 125, and at the top of Fig. 2. We have to stress that the field values indicated in Fig. 3 correspond to the maximum field strength in the cavity holes. The field value in the central part of the cavity is roughly 100 times smaller, and therefore without significance in low-flux maser experiments. Figure 3 also shows that the qualitative structure of the maser line is the same for all fields larger than about 200 mV/cm. Thus, the conditions

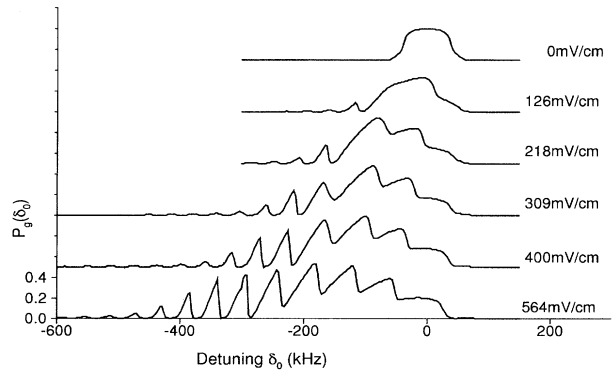

FIG. 3. Theoretical maser lines for the indicated values of the static electric field strength in the cavity holes. The theoretical model is explained in the text. In the calculation we use $N_{\mathrm{ex}} = 100$ and $\Omega = 45$ krad/s. The interaction time is $t_{\mathrm{int}} = 35$ μs, and the rms deviation of the interaction time is 1 μs. In order to account for the fluctuations of the dynamic phases induced by the inhomogeneity of the stray electric fields, a Gaussian distribution of the atom-field detuning with a rms deviation of 5 kHz is assumed (see also Ref. [5]).

required to find the periodic substructures experimentally are not very stringent.

The calculations also reproduce the experimental finding that the maser line shifts to lower frequencies when N_{ex} is increased. The mechanism for that can be explained as follows: the high-frequency edge of the maser line does not shift with N_{ex} at all, since this part of the resonance is produced in the central region of the cavity, where practically no static electric fields are present. The low-frequency cutoff of the structure is determined by the location where the mixing of the dressed states occurs. With decreasing cavity frequency those points shift closer to the entrance and exit holes. Closer to the holes the passage behavior of the atoms through the mixing locations gets nonadiabatic for the following reasons: First, the maser field strength reduces towards the holes. This leads to reduced repulsion of the dressed states. Second, the stray electric field stongly increases towards the holes. This implies a larger differential slope of the dressed state energies at the mixing locations, and therefore leads to a stronger nonadiabatic passage. At the same time the observed signal extends farther to the "red" spectral region. Since the photon emission probabilities β_n are decreasing towards lower frequencies, their behavior finally defines the low-frequency boundary of the maser resonance line. With increasing N_{ex} the photon number n increases. As for larger values of n the photon emission probabilities β_n get larger, also an increasing N_{ex} leads to an extension of the range of the signal to lower frequencies.

The shift of the maser line towards lower frequencies with increasing t_{int} (Fig. 2) also follows from the developed model: The redshift increases with t_{int} since a longer interaction time leads to a more adiabatic behavior in the same way as a larger N_{ex} does.

The calculations reveal that on the vertical steps displayed in the signal the photon number distribution has two distinctly separate maxima. This situation is similar to the conditions discussed in Ref. [5], where maser field hysteresis and metastability are observed. Therefore, the maser field should exhibit hysteresis and metastability under the present conditions as well. The hysteresis should show up when the cavity frequency is linearly scanned up and down with a modest scan rate. An experimental result is given in Fig. 4.

When the maser is operated in steady state and the cavity frequency is fixed to the steep side of one of the fringes, we also observed spontaneous jumps of the maser field between two metastable field states. The results displayed in Fig. 5 show that the maser field jumps between two values, whereby the lower one corresponds to almost zero field. The difference between the photon numbers of the two metastable states can be as low as 25.

The calculations also show that on the smooth wings of the more pronounced interference fringes the photon number distribution $P(n)$ of the maser field is strongly sub-Poissonian. This leads us to the conclusion that we observe Ramsey-type interference induced by a

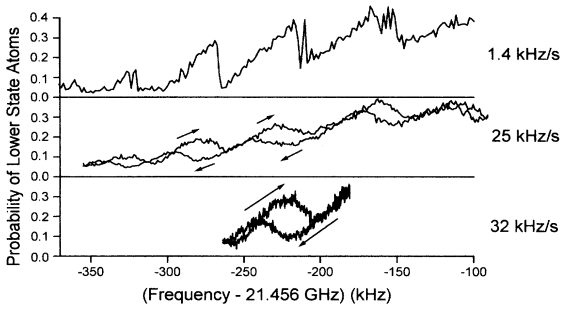

FIG. 4. Hysteresis cycle of the maser for $t_{int} = 35$ μs and $N_{ex} = 84$. Again the atomic inversion is plotted versus the cavity frequency. The upper plot shows a slow scan on the low-frequency wing of the signal. The lower plots show that the vertical steps turn into hysteresis loops when the cavity frequency is rapidly scanned up and down. The values to the right indicate the scan speed.

nonclassical radiation field. The sub-Poissonian character of $P(n)$ results from the fact that on the smooth wings of the fringes the photon gain locally reduces when the photon number is increased. This feedback mechanism stabilizes the photon number resulting in a sub-Poissonian photon distribution.

The presented maser model explains all the observed experimental facts. The periodic structures in the maser lines are interpreted as Ramsey-type interferences. If there was more accurate information on the dc fields in the cavity, a multilevel calculation taking into account the magnetic substructure of the involved fine-structure levels would make sense. Under the present conditions, however, the stray electric field amplitudes close to the cavity holes can only be estimated. The interference structure extends towards lower frequency as far as $\approx$500 kHz for $N_{ex} \approx 200$, this corresponding to an electric field of $\approx$25 mV/cm in a distance of roughly a few mm from the cavity holes.

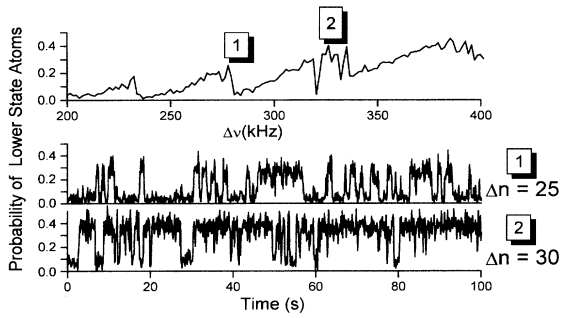

FIG. 5. Spontaneous jumps of the maser field for $t_{int} = 35$ μs and $N_{ex} = 84$. When the maser is operated at locations 1 and 2 of the maser line shown in the upper plot, the atomic inversion as a function of time statistically jumps as displayed in the lower plots. The values Δn denote the differences of the mean photon numbers in the two metastable field states.

In this paper we describe the first observation of Ramsey-type atomic interferometry in the nonclassical field of the micromaser. To our knowledge it is the first time that it is demonstrated that nonadiabatic mixing can lead to Ramsey interferences. Besides other phenomena the bistable character of the micromaser field can be observed in jumps of the interferences; the observed interferences thus show a discontinuous behavior owing to the quantum properties of the field—it is the first time that such a discrete quantum behavior is directly observed in interference fringes. One of the applications of the described Ramsey interferometer could be the quantum-nondemolition measurement of the photon number in a cavity along the lines proposed in Ref. [10]. For this purpose the atoms in the cavity have to be dispersively coupled to a third level via a second quantum field. The second field could be another cavity mode. Assuming that the photon lifetime of the second field is much longer than the photon lifetime corresponding to the maser transition, the number of photons in the second field can be determined from the shift of the interference patterns.

[1] D. Meschede, H. Walther, and G. Müller, Phys. Rev. Lett. **54**, 551 (1985).
[2] G. Rempe, H. Walther, and N. Klein, Phys. Rev. Lett. **58**, 353 (1987).
[3] G. Rempe, F. Schmidt-Kaler, and H. Walther, Phys. Rev. Lett. **64**, 2783 (1990).
[4] G. Rempe and H. Walther, Phys. Rev. A **42**, 1650 (1990).
[5] O. Benson, G. Raithel, and H. Walther, Phys. Rev. Lett. **72**, 3506 (1994).
[6] N. F. Ramsey, *Molecular Beams* (Clarendon Press, Oxford, 1956).
[7] See, for example, C. Cohen-Tannoudji, J. Dupont-Roc, and G. Grynberg, *Atom-Photon Interactions* (John Wiley and Sons, Inc., New York, 1992).
[8] P. Filipowicz, J. Javanainen, and P. Meystre, Phys. Rev. A **34**, 3077 (1986).
[9] L. A. Lugiato, M. O. Scully, and H. Walther, Phys. Rev. A **36**, 740 (1987).
[10] M. Brune, S. Haroche, V. Lefevre, J. M. Raimond, and N. Zagury, Phys. Rev. Lett. **65**, 976 (1990).